

Vibrational dephasing by the exchange mechanism: Some new results

A. Nitzan^{a)} and B. N. J. Persson

Institut für Festkörperforschung der Kernforschungsanlage Jülich, D 5170 Jülich, West Germany

(Received 15 July 1985; accepted 26 August 1985)

The exchange model of vibrational phase relaxation is studied. The vibrational line profile is obtained analytically in various limiting cases such as high temperature and large friction.

Expressions for the first and second moments of the line profile are also presented.

I. INTRODUCTION

Considerable effort has recently been directed towards the understanding of vibrational line shapes at surfaces.¹ For high-frequency vibrations at metal surfaces, both energy relaxation (via excitation of electron hole pairs) and phase relaxation will in general contribute to the linewidth and line shift. For vibrations at insulator surfaces only dephasing is relevant because energy relaxation via multiphonon emission is unimportant for high-frequency vibrations. These conclusions are supported by recent observations and analysis of the temperature dependent widths and shifts of the absorption lines associated with the C–O stretching vibration of CO adsorbed on Ni(111)^{2,3} and Pt(111),⁴ and of the Si–H stretching vibration for H adsorbed on Si(100).⁵

In a recent series of papers, Persson and Ryberg³ and Persson⁶ have presented theoretical calculations of the vibrational line shape [with applications to CO/Ni(111)] based on the exchange model for phase relaxation. This model was proposed by Harris and co-workers⁷ to explain the vibrational line shapes of high-frequency modes of polyatomic impurities in condensed phases.

The physical picture used to describe vibrational dephasing by the exchange mechanism for an adsorbed molecule was described earlier.^{6,7} Briefly, the high-frequency mode interacts with low-frequency local modes such as frustrated translations or frustrated rotations of the adsorbate. The latter are coupled to the lattice phonons. The anharmonic coupling between the high-frequency mode and the low-frequency fluctuating modes is the source of the former's dephasing. The simplest model for this process is described by the Hamiltonian

$$H = \omega_a a^\dagger a + \omega_b b^\dagger b + \delta\omega a^\dagger a b^\dagger b + V, \quad (1)$$

where a is the annihilation operator for the high-frequency mode (of frequency ω_a) under study, b is the annihilation operator for the low-frequency local mode, $\delta\omega$ (the exchange coupling) is a measure of the anharmonic coupling between the A and B modes, and V is the Hamiltonian for the lattice phonons plus their coupling to the low-frequency mode B . Obviously more than one (local) low-frequency mode may be involved but such a slightly more complicated model was not found necessary in actual cases studied so far.

In the model (1), the interaction between the A and B modes was taken to be bilinear in both mode coordinates. In systems where the impurity molecule is located in a site of

high symmetry, such as the CO/Ni(111) system studied in Refs. 3 and 4, this is required by the symmetry of the problem. In less symmetrical situations terms such as $a^\dagger a (b + b^\dagger)$ will also appear. Shelby *et al.*^{7(b)} have argued that the symmetric term appearing in Eq. (1) is more important even in such cases, but their argument is based on the assumption that the coefficients of expansion of the interaction potential which yield these (and higher order terms) are all of the same magnitude. Such an assumption usually does not hold. Nevertheless, we focus our discussion in this paper on the symmetric model (1) which is the appropriate model for most line shape problems involving adsorbed molecules. The case where the term $\delta\omega a^\dagger a b^\dagger b$ in Eq. (1) is replaced by $\delta\omega a^\dagger a (b + b^\dagger)$ is actually easier to solve analytically and its implications are discussed at the end of the paper.

When the B mode–lattice coupling occurring in V vanishes, the transition $0 \rightarrow 1$ between the ground and the first excited level of the A mode has (at finite temperature) superimposed on it more lines associated with the different populations of the B mode, i.e., the lines $0n \rightarrow 1n$ ($n = 0, 1, \dots$), where the first number refers to the high and the second to the low-frequency mode populations. If, e.g., $\delta\omega$ is positive these lines lie on the high-frequency side of the main $00 \rightarrow 10$ line and their intensities are proportional to the thermal populations of the corresponding B states. In a real system, even without the effect of V , these lines will be inhomogeneously broadened and, for adsorbates on metal surfaces, additionally broadened by the e – h pair production mechanism. These contributions to the total width are essentially temperature independent. The presence of V leads to an additional temperature dependent shift and broadening associated with the indirect coupling (via the B mode) of the A mode to the lattice phonons.

It is clear from the above discussion (see also Refs. 6 and 7) that in general the absorption line associated with the high-frequency mode A will be asymmetric, and for small enough friction ($\delta\omega \gg \eta$; the friction η determines the damping of the low-frequency mode B due to emission of lattice phonons), it will consist of several nonoverlapping peaks. Analysis of the experimental line shape may be carried out either (a) by considering the total absorption profile, e.g., by evaluating its moments, or (b) by focusing on the main peak characterized by, e.g., its center frequency (the frequency of maximum absorption) and by its linewidth (e.g., the full width at half-maximum, FWHM). The first approach is often difficult or impossible to carry out in practice because a substantial part of the total intensity may be imbedded in the noise. This is particularly serious when evaluating higher

^{a)}Permanent address: Department of Chemistry, Tel-Aviv University, Tel-Aviv, Israel.

moments such as $\langle(\omega - \langle\omega\rangle)^2\rangle$ where an accurate knowledge of the “wings” of the absorption spectra is necessary. For this reason the experimental data reported in Ref. 3 were presented as center frequency and linewidth (FWHM).

In the present article we consider both possibilities (a) and (b). The total line shape analysis is done by calculating the first and second moments of the absorption associated with the high-frequency mode within the model (1). The results are obtained in terms of sum rules, and the same method is capable of yielding moments of any desired order. Main peak analysis is done by considering the long time limit of the dipole–dipole correlation function whose Fourier transform is the line shape.

In the next section, we calculate the absorption line shape associated with mode *A* in the model (1), using a cumulant expansion and taking the long time limit in calculating the dipole–dipole correlation function. This leads to a Lorentzian line shape with width and shift in agreement with results obtained earlier using other methods. This calculation serves to show that the long time limit of the dipole correlation function indeed contains the information needed to characterize the Lorentzian center of the peak. It is also shown that a truncated cumulant expansion corresponds to the high friction limit ($\eta > \delta\omega$) of the model.

In some situations a full quantum mechanical analysis is not necessary. When $\omega_b < k_B T$ a classical analog of the Hamiltonian (1) is sufficient, provided that in addition the peaks corresponding to the different $0n \rightarrow 1n$ ($n = 0, 1, \dots$) transitions overlap. In Secs. III and IV we calculate the line shape associated with the classical analog of Eq. (1):

$$\ddot{x}_a + \omega_a^2 x_a + \alpha x_b^2 x_a = 0, \tag{2}$$

$$\ddot{x}_b + \omega_b^2 x_b + \alpha(m_a/m_b)x_a^2 x_b + \eta \dot{x}_b = f(t), \tag{3}$$

where $\alpha \sim \delta\omega$ and where the random force $f(t)$, in accordance with the fluctuation dissipation theorem, satisfies

$$\langle f(t) f(0) \rangle = (2\eta k_B T / m_b) \delta(t). \tag{4}$$

Using this model, in Sec. III we calculate the long time limit of the classical dipole–dipole correlation function using an infinite order cumulant expansion. In Sec. IV, we obtain the same results by taking the classical limit of the full quantum mechanical solution of Ref. 3.

In Sec. V, we evaluate sum rules which correspond to the moments of the absorption line shape. We show that if a shift and a width are calculated from the first and second moments, the results are different from those calculated from the center peak analysis of the earlier sections, stressing again that the Lorentzian shape is valid only in a limited region near the main peak.

We conclude this paper with some numerical examples and a discussion of the results obtained.

II. THE QUANTUM CASE

Here we present a derivation of the linewidth and shift associated with the exchange dephasing model described above. While the present treatment is limited to large friction, $\eta > \delta\omega$, it provides in this limit analytical results which holds for all temperatures, thus extending the results of earlier work. Our starting point is the Hamiltonian

$$H = \omega_a a^+ a + \bar{\omega}_b b^+ b + \delta\omega a^+ a b^+ b + \sum_k \omega_k c_k^+ c_k + \sum_k (V_k c_k^+ b + V_k^* c_k b^+), \tag{5}$$

where a, a^+, b, b^+ , and c_k, c_k^+ are annihilation and creation operators for the high-frequency, the low-frequency, and the thermal bath modes, respectively. Their time evolution is determined by the following equations of motion:

$$\dot{a} = -i\omega_a a - i\delta\omega a b^+ b, \tag{6}$$

$$\dot{b} = -i\bar{\omega}_b b - i\delta\omega \hat{n}_a b - i \sum_k V_k^* c_k, \tag{7}$$

$$\dot{c}_k = -i\omega_k c_k - iV_k b. \tag{8}$$

Here $\hat{n}_a = a^+ a$ is an operator, but under the Hamiltonian (5) it is a constant of the motion and will be regarded as a number in solving Eqs. (7) and (8). Denoting

$$\omega_b = \bar{\omega}_b + \delta\omega \hat{n}_a + \text{Re} \sum_k \frac{|V_k|^2}{\omega - \omega_k + i\epsilon} \quad (\epsilon \rightarrow 0). \tag{9}$$

The solution of Eqs. (7) and (8) is obtained in the form

$$b(t) = F(t)b(0) + \sum_k F_k(t)c_k(0) \tag{10}$$

with

$$F(t) = e^{-i\omega_b t - \frac{1}{2}\Gamma_b t}, \tag{11}$$

$$F_k(t) = \frac{V_k^* e^{-i\omega_k t}}{\omega_k - \omega_b + \frac{1}{2}i\Gamma_b} (1 - e^{-i(\omega_b - \omega_k)t - \frac{1}{2}\Gamma_b t}), \tag{12}$$

$$\Gamma_b = 2\pi (|V_k|^2 \rho_k)_{\omega_k = \omega_b}. \tag{13}$$

Note that $F(t)$ and $F_k(t)$ satisfy

$$|F(t)|^2 + \sum_k |F_k(t)|^2 = 1. \tag{14}$$

Also note that in Eqs. (11) and (12) we have assumed that $\Gamma_b = 2\pi |V_k|^2 \rho_k$ is a weak function of ω_k .

The line shape associated with the high-frequency mode may be written as

$$L(\omega) = \frac{2}{1 - e^{-\beta\hbar\omega}} \text{Re} \int_0^\infty dt e^{i\omega t} \langle [a(t), a^+(0)] \rangle, \tag{15}$$

$a(t)$ is the solution of the Heisenberg equation (6). In this equation, $b^+(t)b(t)$ depends on a through the \hat{n}_a dependence of ω_b , Eq. (9). A simple solution is obtained if we approximate \hat{n}_a by its thermal average $\langle n_a \rangle$. In most relevant cases, $\hbar\omega_a \gg k_B T$ and $\langle n_a \rangle \simeq 0$.

Inserting the solution of Eq. (6),

$$a(t) = \exp \left[-i\omega_a t - i \int_0^t d\tau \hat{\omega}_1(\tau) \right] a(0) \tag{16}$$

into Eq. (15), we get

$$L(\omega) = \frac{2}{1 - e^{-\beta\hbar\omega}} \text{Re} \int_0^\infty dt e^{i(\omega - \omega_a)t} \langle e^{-i \int_0^t d\tau \hat{\omega}_1(\tau)} \rangle, \tag{17}$$

where

$$\hat{\omega}_1 = \delta\omega b^+(\tau)b(\tau). \tag{18}$$

This evaluation of the average

$$I(t) = \langle \exp(-i \int_0^t d\tau \hat{\omega}_1(\tau)) \rangle \tag{19}$$

is outlined in Appendix A. In performing this average we first calculate the thermal average over the c modes using second order cumulant expansion. The result is then a function of the b, b^+ operators. In the light of the discussion of the preceding section, we are interested in the $\langle 0_b | \dots | 0_b \rangle$ component of this function (0_b denotes the ground state of the low-frequency mode) which corresponds to the line shape associated with the 0_b-0_b component of the 0_a-1_a transition.

The result of the calculation of Appendix A is

$$I(t) = \exp[K_1(t) + \frac{1}{2}K_2(t)], \quad (20)$$

where

$$K_1(t) \cong -i\delta\omega n_b t, \quad (21)$$

$$\frac{1}{2}K_2(t) \cong -\delta\omega^2 \frac{n_b(n_b+1)}{\Gamma_b} t, \quad (22)$$

and where

$$n_b = \frac{1}{e^{\beta\hbar\omega_b} - 1}. \quad (23)$$

From Eq. (17) we now get

$$L(\omega) \sim \frac{\delta\omega^2 n_b(n_b+1)/\Gamma_b}{[\omega - (\omega_a + \delta\omega n_b)]^2 + [n_b(n_b+1)\delta\omega^2/\Gamma_b]^2}, \quad (24)$$

a Lorentzian with shift $\Delta\omega$ and width Γ given by

$$\Delta\omega = \delta\omega n_b, \quad (25)$$

and

$$\Gamma = 2n_b(n_b+1)\delta\omega^2/\Gamma_b. \quad (26)$$

These results are generalizations, valid for all temperatures, of the previously obtained shift and width in the high friction ($\Gamma_b > \delta\omega$) limit. That the low order cumulant expansion corresponds to this limit results from it being an expansion in powers of functions of the form $\delta\omega \int' d\tau f(\tau)$, where $f(\tau)$ decays exponentially like $e^{-\Gamma_b \tau}$.

III. HIGH TEMPERATURE EXPANSION (I)

In this section we derive expression for the linewidth and shift associated with the classical analog of Eq. (1), namely,

$$\ddot{x}_a + \omega_a^2 x_a + \alpha x_b^2 x_a = 0, \quad (27a)$$

$$\ddot{x}_b + \bar{\omega}_b^2 x_b + \alpha(m_a/m_b)x_a^2 x_b + \eta \dot{x}_b = f(t) \quad (27b)$$

with $\langle f \rangle = 0$ and

$$\langle f(t)f(0) \rangle = c\delta(t); \quad c = \frac{2\eta k_B T}{m_b}. \quad (28)$$

a denotes the high-frequency mode and b the low-frequency mode. α is related to $\delta\omega$ of Eq. (1) by

$$\alpha = \frac{2m_b \bar{\omega}_b \omega_a}{\hbar} \delta\omega. \quad (29)$$

The line shape associated with the a mode is

$$L(\omega) \propto \int_{-\infty}^{\infty} dt e^{i\omega t} \langle x_a(t)x_a(0) \rangle. \quad (30)$$

To get $x_a(t)$ we first solve Eq. (27b) for $x_b(t)$. Since $\omega_a \gg \bar{\omega}_b$ we

replace x_a^2 in Eq. (27b) by its average $\langle x_a^2 \rangle = k_B T/m_a \omega_a^2$. Defining

$$\omega_b^2 = \bar{\omega}_b^2 + \alpha \frac{m_a}{m_b} \langle x_a^2 \rangle, \quad (31)$$

we now have the simple Langevin equation for the motion of the low-frequency mode

$$\ddot{x}_b + \omega_b^2 x_b + \eta \dot{x}_b = f \quad (32)$$

which is easily solved in Fourier space to yield

$$\hat{x}_b(\omega) = \frac{\hat{f}(\omega)}{\omega_b^2 - \omega^2 - i\omega\eta}, \quad (33)$$

$$\langle \hat{x}_b(\omega)\hat{x}_b(\omega') \rangle = \frac{2\pi c}{(\omega_b^2 - \omega^2)^2 + \omega^2\eta^2} \delta(\omega + \omega'), \quad (34)$$

where

$$\hat{f}(\omega) = \int_{-\infty}^{\infty} dt e^{i\omega t} f(t)$$

and

$$\hat{x}(\omega) = \int_{-\infty}^{\infty} dt e^{i\omega t} x(t).$$

Equation (34) leads to

$$\langle x_b(t)x_b(t') \rangle = \frac{c}{2\pi} \int_{-\infty}^{\infty} d\omega e^{-i\omega(t-t')} \times \frac{1}{(\omega_b^2 - \omega^2)^2 + \omega^2\eta^2}. \quad (35)$$

$x_b(t)$ is now regarded as a stochastic term in Eq. (27a), whose statistical properties are given by Eqs. (34) and (35). Solving Eq. (27a) using the WKB approximation⁸ we get

$$x_a(t) = x_a(0) \exp\left[-i\omega_a t - i\frac{\alpha}{2\omega_a} \int_0^t d\tau x_b^2(\tau)\right]. \quad (36)$$

Inserting into Eq. (30) we now get

$$L(\omega) \propto \int_{-\infty}^{\infty} dt e^{i(\omega - \omega_a)t} I(t), \quad (37)$$

where

$$I(t) = \langle \exp\left[-i\frac{\alpha}{2\omega_a} \int_0^t d\tau x_b^2(\tau)\right] \rangle. \quad (38)$$

This average is evaluated in the long time limit in Appendix B. The result is

$$I(t) = e^{-i\Delta\omega t - \frac{1}{2}\Gamma|t|} \quad (t \rightarrow \infty), \quad (39)$$

where

$$\Delta\omega = \frac{1}{4\pi} \int_{-\infty}^{\infty} d\omega \arctan\left[\frac{\alpha}{\omega_a} \hat{Z}(\omega)\right], \quad (40)$$

$$\Gamma = \frac{1}{4\pi} \int_{-\infty}^{\infty} d\omega \ln\left[1 + \left[\frac{\alpha}{\omega_a} \hat{Z}(\omega)\right]^2\right], \quad (41)$$

and where

$$\hat{Z}(\omega) = \frac{c}{(\omega_b^2 - \omega^2)^2 + \omega^2\eta^2}. \quad (42)$$

The long time limit used to obtain Eq. (39) is relevant if we are interested in the line shape near the center $\omega \sim \omega_a + \Delta\omega$. This is indeed the case in the light of the discussion of Sec. I.

In this approximation the line shape is a Lorentzian,

$$L(\omega) \propto \frac{1/2\Gamma}{[\omega - (\omega_a + \Delta\omega)]^2 + (\frac{1}{2}\Gamma)^2} \quad (43)$$

with $\Delta\omega$ and Γ corresponding to the frequency shift and the width (FWHM). Equations (40) and (41) are easily integrated numerically. They can also be evaluated analytically by first integrating by parts to get

$$\Delta\omega = -\frac{\alpha}{4\pi\omega_a} \int_{-\infty}^{\infty} d\omega \frac{\omega \hat{Z}'(\omega)}{1 + [\alpha/\omega_a \hat{Z}(\omega)]^2}, \quad (44)$$

$$\Gamma = -\frac{\alpha^2}{2\pi\omega_a^2} \int_{-\infty}^{\infty} d\omega \frac{\omega \hat{Z}'(\omega) \hat{Z}(\omega)}{1 + [(\alpha/\omega_a) \hat{Z}(\omega)]^2} \quad (45)$$

and then proceeding with complex integration along a contour circling the upper or lower complex ω plane. As a simplified version of this procedure consider the case $\eta \ll \omega_b$. For this case $\hat{Z}(\omega)$ may be approximated by⁹

$$\hat{Z}(\omega) \sim \frac{c/(2\omega_b^2)}{(\omega - \omega_b)^2 + (\eta/2)^2}. \quad (46)$$

From Eqs. (44) and (45) with $Z(\omega)$ given by Eq. (46) we get

$$\Delta\omega = \frac{\eta}{2\sqrt{2}} \left[\left(1 + \left[\frac{4\delta\omega n_b}{\eta} \right]^2 \right)^{1/2} - 1 \right]^{1/2}, \quad (47)$$

$$\Gamma = \eta \left[\frac{1}{\sqrt{2}} \left(1 + \left[1 + \left(\frac{4\delta\omega n_b}{\eta} \frac{\bar{\omega}_b}{\omega_b} \right)^2 \right]^{1/2} \right)^{1/2} - 1 \right], \quad (48)$$

where

$$n_b \equiv \frac{kT}{h\omega_b} \quad (49)$$

is the classical limit of the thermal population of the low-frequency mode and where we have used Eq. (29) to express α in terms of $\delta\omega$.

The results (47) and (48) are limited to the (common) situation where $\eta \ll \omega_b$. In the opposite limit, $\eta \gg \omega_b$, the low-frequency mode is overdamped. In this case, the contribution to the integrals (40) and (41) comes mainly from $\omega \sim 0$ and $\hat{Z}(\omega)$, Eq. (42), may be approximated by

$$\hat{Z}(\omega) \sim \frac{c}{\omega_b^4 + \omega^2 \eta^2}. \quad (50)$$

Evaluating the integral (45) with $\hat{Z}(\omega)$ given by Eq. (50) we get

$$\Gamma = \frac{\omega_b^2}{\eta} \left\{ \frac{1}{\sqrt{2}} \left[1 + \left(1 + \left[\frac{4\delta\omega n_b \eta}{\omega_b^2} \frac{\bar{\omega}_b}{\omega_b} \right]^2 \right)^{1/2} \right]^{1/2} - 1 \right\} \quad (\eta/\omega_b \rightarrow \infty). \quad (51)$$

We should keep in mind, however, that in this limit the line shape is not a Lorentzian and the long time limit inherent in Eq. (39) no longer applies. In fact, Eq. (51) vanishes as $\eta^{-1/2}$ as $\eta \rightarrow \infty$, while from Eq. (26) we expect in this limit a Gaussian line shape associated with the thermal distribution of the effective frequency $\bar{\omega}_a^2 = \omega_a^2 + \alpha x_b^2$.

IV. HIGH TEMPERATURE EXPANSION (II)

In this section, we will present an alternative theoretical treatment of the high temperature line shape problem. Within the Markoff approximation the vibrational line shape $I(\omega)$

is accurately given by the following result, valid for any temperature⁶:

$$I(\omega) \sim -\text{Im } D(\omega), \quad (52)$$

$$D(\omega) = \sum_{n,m=0}^{\infty} D_{nm}(\omega), \quad (53)$$

where the matrix D_{nm} satisfies

$$\begin{aligned} (\omega - \omega_a - m\delta\omega)D_{nm} + i\eta(2mn_b + m + n_b)D_{nm} \\ - i\eta(m+1)(n_b+1)D_{n,m+1} - i\eta mn_b D_{n,m-1} \\ = \delta_{nm} e^{-\beta n \omega_b} (1 - e^{-\beta \omega_b}), \end{aligned} \quad (54)$$

where

$$n_b = (e^{\beta \omega_b} - 1)^{-1}$$

is the Bose-Einstein factor for the low-frequency mode. For large temperatures

$$n_b \approx k_B T / \omega_b \gg 1$$

and the main contribution to the sum $\sum_{nm} D_{nm}$ comes from large n and m ($n \sim m \sim n_b$). Thus we can treat n and m as continuous variables and write

$$D_{n,m \pm 1} \rightarrow D_{nm} \pm \frac{\partial}{\partial m} D_{nm} + \frac{1}{2} \frac{\partial^2}{\partial m^2} D_{nm}. \quad (55)$$

Substituting Eq. (55) in Eq. (54) gives

$$\begin{aligned} (\omega - \omega_a - m\delta\omega - i\eta)D_{nm} - i\eta(n_b + m) \frac{\partial}{\partial m} D_{nm} \\ - i\eta n_b m \frac{\partial^2}{\partial m^2} D_{nm} = \delta(n - m) e^{-\beta m \omega_b / n_b}. \end{aligned}$$

Next, we integrate over n and introduce

$$x = m/n_b, \quad G(x) = -i\eta n_b \int_0^{\infty} dn D_{nm}.$$

We get

$$xG'' + (1+x)G' + i(a+bx)G = e^{-x}, \quad (56)$$

where $a = (\omega - \omega_a - i\eta)/\eta$, $b = -n_b \delta\omega/\eta$, and $G' = \partial G / \partial x$. The line shape is given by

$$I(\omega) \sim -\text{Im} \int_0^{\infty} dn dm D_{nm}(\omega) = -\frac{1}{\eta} \text{Re} \int_0^{\infty} dx G(x, \omega). \quad (57)$$

The differential equation (56) is solved in Appendix C where it is shown that

$$\begin{aligned} I(\omega) \sim -\text{Im} \left\{ \frac{4w}{(1+w)^2} \sum_{n=0}^{\infty} \left(\frac{1-w}{1+w} \right)^{2n} \right. \\ \left. \times \left[\frac{1}{\omega - \omega_a - \Delta\omega_n + i\Gamma_n/2} \right] \right\}, \end{aligned} \quad (58)$$

where

$$w = (1 + 4in_b \delta\omega/\eta)^{1/2}$$

and where

$$\Delta\omega_n = \pm (2n+1) \frac{\eta}{2\sqrt{2}} \left[\left(1 + \left[\frac{4\delta\omega n_b}{\eta} \right]^2 \right)^{1/2} - 1 \right]^{1/2}, \quad (59)$$

$$\Gamma_n = \eta \left[\frac{2n+1}{\sqrt{2}} \left(1 + \left[\left(\frac{4\delta\omega n_b}{\eta} \right)^2 \right]^{1/2} \right)^{1/2} - 1 \right]. \quad (60)$$

In expression (59), the \pm sign is determined by the sign of $\delta\omega$. The $n = 0$ terms in these expressions are identical to the results of Sec. III. The contribution from the other terms ($n = 1, 2, \dots$) can in many cases be neglected (see Sec. VI).

V. MOMENTS OF THE LINE SHAPE

The line shape $L(\omega)$ can be written as

$$L(\omega) = \frac{1}{2\pi} \int_{-\infty}^{\infty} dt e^{i\omega t} \langle a(t) a^+(0) \rangle.$$

Thus,

$$\int d\omega e^{-i\omega t} L(\omega) = \langle a(t) a^+(0) \rangle.$$

Expanding both sides in power of t gives

$$\begin{aligned} \int d\omega L(\omega) - it \int d\omega L(\omega) \omega - \frac{t^2}{2} \int d\omega L(\omega) \omega^2 + \dots \\ = \langle a(0) a^+(0) \rangle + t \langle \dot{a}(0) a^+(0) \rangle + \frac{1}{2} t^2 \langle \ddot{a}(0) a^+(0) \rangle + \dots \end{aligned}$$

Thus,

$$\int d\omega L(\omega) = \langle a(0) a^+(0) \rangle \approx 1,$$

$$\int d\omega L(\omega) \omega \equiv \langle \omega \rangle = i \langle \dot{a}(0) a^+(0) \rangle = \langle [a, H] a^+ \rangle,$$

and

$$\langle \omega^2 \rangle = \langle [[a, H], H] a^+ \rangle.$$

Using Eq. (5) we calculate

$$[a, H] = (\omega_a + \delta\omega \hat{n}_b) a, \quad (61)$$

so that

$$\langle \omega \rangle = \omega_a + \delta\omega \langle \hat{n}_b \rangle.$$

The frequency shift $\langle \omega \rangle - \omega_a = \delta\omega \langle \hat{n}_b \rangle$ agree with the result (25) which is valid in the large friction limit. This result is expected since, in the large friction limit, $L(\omega)$ is a Lorentzian and for a symmetric peak the center frequency (i.e., the frequency at peak maximum) must coincide with the center of mass $\langle \omega \rangle$ of the distribution $L(\omega)$. However, this is no longer true if the absorption peak is asymmetric (as is generally the case) and, indeed, $\langle \omega \rangle - \omega_a$ differs from Eq. (47).

Next, to obtain $\langle \omega^2 \rangle$ we must evaluate $[[a, H], H]$. Using Eqs. (5) and (61) we obtain

$$[[a, H], H] = (\omega_a + \delta\omega \hat{n}_b)^2 a - \sum_k (V_k c_k^+ b - V_k^* c_k b^+) \delta\omega a.$$

Thus,

$$\begin{aligned} \langle (\omega - \langle \omega \rangle)^2 \rangle \\ = \delta\omega^2 (\langle \hat{n}_b^2 \rangle - \langle \hat{n}_b \rangle^2) - \sum_k \delta\omega \langle V_k c_k^+ b - V_k^* c_k b^+ \rangle. \end{aligned}$$

The quantity $(\langle (\omega - \langle \omega \rangle)^2 \rangle)^{1/2}$, which is a measure of the peak width, differs from both Eqs. (26) and (48) and is therefore not related in any simple way to the full width at half-maximum of $L(\omega)$.

VI. NUMERICAL RESULTS AND DISCUSSION

According to Eq. (58) the high temperature line profile is a sum of Lorentzians with different width Γ_n and frequency

shift $\Delta\omega_n$. The weight of each Lorentzian is proportional to x^n where

$$x = \left(\frac{1-w}{1+w} \right)^2.$$

In Fig. 1, we show $|x|$ as a function of $\delta\omega n_b / \eta = \delta\omega k_B T / \eta \omega_b$. Obviously, $|x| < 1$ so that the series (58) converges. Furthermore, the FWHM = Γ and the frequency shift $\Delta\omega$ of the absorption peak $I(\omega)$ are approximately determined by the first (i.e., $n = 0$) term in the expansion (58):

$$\Gamma \approx \eta \left[\frac{1}{\sqrt{2}} \left(1 + \left[1 + \left(\frac{4\delta\omega n_b}{\eta} \right)^2 \right]^{1/2} \right)^{1/2} - 1 \right], \quad (59b)$$

$$\Delta\omega \approx \frac{\pm \eta}{2\sqrt{2}} \left[\left(1 + \left[\frac{4\delta\omega n_b}{\eta} \right]^2 \right)^{1/2} - 1 \right]^{1/2}. \quad (60b)$$

The reason for this to hold approximately is that the higher order terms ($n = 1, 2, \dots$) in the expansion (58) have a much larger damping and smaller weight $\sim |x|^n$. This is illustrated in Fig. 2 which shows the line profile for $\delta\omega = \eta = 10 \text{ cm}^{-1}$ and $n_b = 5$. The dashed curves are calculated from the high temperature expansion (58) by summing over $n = 0, 1, \dots$ (upper curve) and by excluding the $n = 0$ contribution (lower curve). The latter curve forms a weak and slowly varying "backgrounds" which obviously has quite a small influence on the peak width and position, as claimed above. In Fig. 2 we also show the "exact" line profile as obtained by solving Eqs. (52)–(54) numerically.

In Fig. 3 we show how the peak width Γ and the frequency shift $\Delta\omega$ vary with the temperature for a case where $\delta\omega = \eta = 10 \text{ cm}^{-1}$ and $\omega_b = 100 \text{ K}$. The full lines are the exact results, Eqs. (52)–(54), while the dashed-dotted lines are the low temperature results of Harris *et al.*⁷:

$$\Gamma = 2e^{-\beta\omega_b} \eta \frac{\delta\omega^2}{\delta\omega^2 + \eta^2}, \quad (62)$$

$$\Delta\omega = e^{-\beta\omega_b} \delta\omega \frac{\eta^2}{\delta\omega^2 + \eta^2}. \quad (63)$$

We close this section by discussing some limiting results for Γ and $\Delta\omega$. For large friction, Eqs. (59b) and (60b) reduce to

$$\Gamma \approx \frac{2\delta\omega^2}{\eta} (k_B T / \omega_b)^2,$$

$$\Delta\omega \approx \delta\omega (k_B T / \omega_b)$$

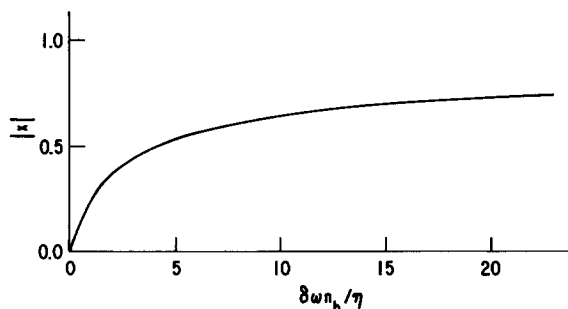


FIG. 1. The function $|x| = |(1-w)/(1+w)|^2$ where $w = (1 + 4in_b\delta\omega/\eta)^{1/2}$.

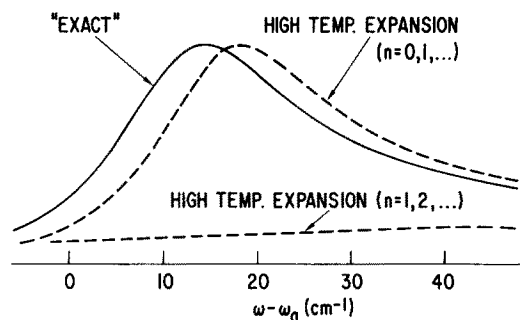


FIG. 2. Full lines: The exact absorption spectra obtained from Eqs. (52)–(54). The dashed lines are obtained from the high temperature expansion (58) by summing over $n = 0, 1, \dots$ (upper curve) and over $n = 1, 2, \dots$ (lower curve). In the calculation we have used $\delta\omega = \eta = 10 \text{ cm}^{-1}$ and $\omega_0 = 100 \text{ cm}^{-1}$ and such a temperature that $n_b = (\exp[\omega_0/k_B T] - 1)^{-1} = 5$.

which agree with earlier results. For $\delta\omega n_b/\eta \gg 1$ we get a drastically different temperature dependence, namely

$$\Gamma = 2|\Delta\omega| = \sqrt{2\eta\delta\omega k_B T/\omega_b} - \eta.$$

Although the various limiting formulas for the linewidth and frequency shift, which we have presented above, should provide useful estimates, for an accurate comparison of theory with experiment one must use the full quantum mechanical solution described at the beginning of Sec. IV.

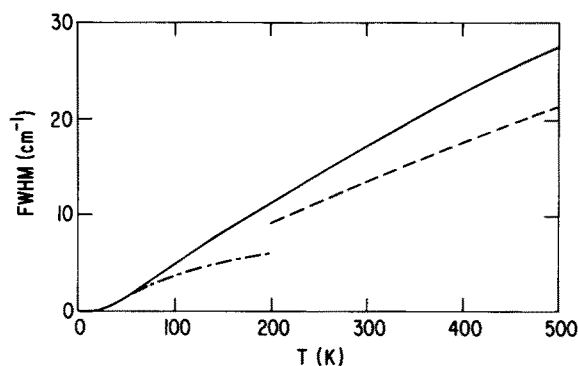
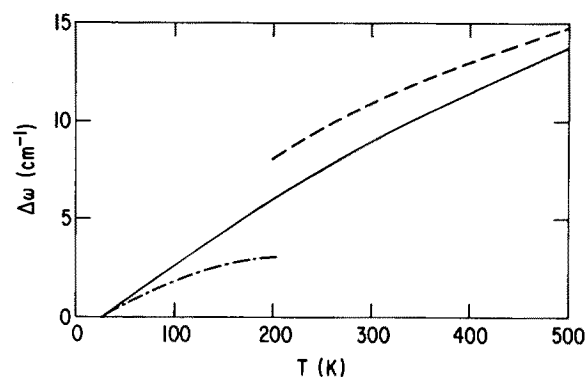


FIG. 3. The frequency shift $\Delta\omega$ and the linewidth (FWHM) as a function of temperature. In the calculations $\delta\omega = \eta = 10 \text{ cm}^{-1}$ and $\omega_0 = 100 \text{ cm}^{-1}$. The full lines are calculated using Eqs. (52)–(54). The dashed lines are obtained from Eqs. (59b) and (60b). The dash-dotted lines are the low temperature expansions (62) and (63).

VII. SUMMARY AND CONCLUSION

The exchange model for vibrational phase relaxation has been shown to explain a large amount of experimental data for vibrations in solids and at surfaces and this motivated the rather detailed study presented in this paper. The main ingredient in the exchange model is an anharmonic coupling V between the high-frequency mode A under study and a low-frequency mode B . In this work $V \sim x_a^2 x_b^2$. In systems where the “impurity” molecule is located in a site of high symmetry, such as the CO/Ni(111) system, this is the lowest nonvanishing anharmonic coupling. In less symmetric situations terms such as $V \sim x_a^2 x_b$ will also appear. One can show that in this case the frequency shift $\Delta\omega$ vanishes (i.e., the temperature independent) while the linewidth increases linearly with temperature (for large temperature and friction). These results should be contrasted with those of Eqs. (25) and (26) which exhibit $\Delta\omega \sim T$ and $\Gamma \sim T^2$ (again for large temperature and friction). The different temperature dependence can be used to distinguish between the different cases ($V \sim x_a^2 x_b^2$ and $x_a^2 x_b$) and therefore also, at least in principle, to derive information about bonding site symmetry.

ACKNOWLEDGMENT

We thank G. Eilenberger for his substantial contribution to this work.

APPENDIX A

Here we evaluate the average $I(t) = \langle \exp(-i\int_0^t d\tau \hat{\omega}_1(\tau)) \rangle$, Eq. (15), where $\hat{\omega}_1$ is given by Eqs. (18) and (10)–(13). We first perform the average over the thermal bath (c) modes. The resulting average is denoted $\bar{I}_c(t)$:

$$I_c(t) = \exp\left[-i\delta\omega \int_0^t d\tau |F(\tau)|^2 b^+ b\right] \bar{I}_c(t), \quad (\text{A1})$$

$$\bar{I}_c(t) = \left\langle \exp -i \int_0^t d\tau \bar{\omega}_1(\tau) \right\rangle_c, \quad (\text{A2})$$

$$\begin{aligned} \bar{\omega}_1(\tau) = & \left\{ F(\tau) \sum_k F_k^*(\tau) b^+ c_k + \text{c.c.} \right. \\ & \left. + \sum_{k_1, k_2} F_{k_1}^*(\tau) F_{k_2}(\tau) c_{k_1}^+ c_{k_2} \right\} \delta\omega. \end{aligned} \quad (\text{A3})$$

$\langle \rangle_c$ denotes thermal averaging over the c modes. To obtain $I(t)$ from $I_c(t)$ we need to average over the thermal population of the b mode

$$I(t) = (1 - e^{-\beta\hbar\omega_b})^{-1} \sum_{n_b=0}^{\infty} e^{-\beta\hbar\omega_b n_b} \langle n_b | I_c(t) | n_b \rangle. \quad (\text{A4})$$

In the spirit of the discussion in the Introduction, we consider only the term $n_b = 0$ which corresponds to the $0_b - 0_b$ component of the $0_a - 1_a$ transition.

We now seek an expression for $\bar{I}_c(t)$ in form of a cumulant expansion

$$\bar{I}_c(t) = e^{K_1(t) + \frac{1}{2}K_2(t) + \dots}. \quad (\text{A5})$$

The first cumulant

$$K_1 = -i \int_0^t d\tau \langle \bar{\omega}_1(\tau) \rangle_c \quad (\text{A6})$$

is easily evaluated to give

$$K_1 \simeq -i\delta\omega n_b \left(t - \frac{1 - e^{-\Gamma_b t}}{\Gamma_b} \right), \quad (\text{A7})$$

where

$$n_b = (e^{\hbar\omega_b/k_B T} - 1)^{-1}$$

and where we have used Eqs. (11) and (14). Note that even though we focus on the $n_b = 0$ term in Eq. (A4), n_b appears in Eq. (A7). This n_b results from terms such as $\langle c_k^\dagger c_k \rangle_c$ calculated for $\omega_k \simeq \omega_b$ as imposed by the weighting function $F_k(t)$, Eq. (12).

The second cumulant

$$K_2 = - \int_0^t d\tau_1 \int_0^t d\tau_2 [\langle \bar{\omega}_1(\tau_1) \bar{\omega}_1(\tau_2) \rangle - \langle \bar{\omega}_1(\tau_1) \rangle \langle \bar{\omega}_1(\tau_2) \rangle] \quad (\text{A8})$$

is also obtained from a straightforward, though lengthy, calculation. As an example consider one of the terms that contribute to Eq. (A8), this arising from the $b^\dagger c_k$ terms of Eq. (A3):

$$\begin{aligned} & \int_0^t d\tau_1 \int_0^t d\tau_2 \left\{ F(\tau_1) F^*(\tau_2) b^\dagger b \sum_k F_k^*(\tau_1) F_k(\tau_2) (\bar{n}_k + 1) \right. \\ & \quad \left. + F^*(\tau_1) F(\tau_2) (b^\dagger b + 1) \sum_k F_k(\tau_1) F_k^*(\tau_2) \bar{n}_k \right\} \quad (\text{A9}) \\ & \simeq \int_0^t d\tau_1 \int_0^t d\tau_2 \left\{ F(\tau_1) F^*(\tau_2) (\bar{n}_b + 1) b^\dagger b s^*(\tau_1, \tau_2) \right. \\ & \quad \left. + F^*(\tau_1) F(\tau_2) \bar{n}_b (b^\dagger b + 1) s(\tau_1, \tau_2) \right\}, \end{aligned}$$

where

$$s(\tau_1, \tau_2) = \sum_k F_k(\tau_1) F_k^*(\tau_2). \quad (\text{A10})$$

s may be evaluated from Eq. (12). The result is

$$s(\tau_1, \tau_2) = e^{-i\omega_b(\tau_1 - \tau_2)} (e^{-\Gamma_b/2|\tau_1 - \tau_2|} - e^{-\Gamma_b/2(\tau_1 + \tau_2)}). \quad (\text{A11})$$

Inserting Eq. (A11) into Eq. (A9) and performing the τ_1 and τ_2 integrations using also Eq. (11) lead to

$$\begin{aligned} (\text{A9}) &= [(2\bar{n}_b + 1) b^\dagger b + \bar{n}_b] \\ & \times \left[2 \frac{1 - e^{-\Gamma_b t}}{\Gamma_b^2} - \frac{2te^{-\Gamma_b t}}{\Gamma_b} - \left(\frac{1 - e^{-\Gamma_b t}}{\Gamma_b} \right)^2 \right]. \quad (\text{A12}) \end{aligned}$$

Other terms contributing to K_2 are evaluated in a similar way. The final result is (replacing $b^\dagger b$ by 0)

$$\begin{aligned} K_2 &= -\delta\omega^2 \left\{ \frac{2\bar{n}_b(\bar{n}_b + 1)}{\Gamma_b} \left(t - \frac{1 - e^{-\Gamma_b t}}{\Gamma_b} \right) \right. \\ & \left. + \bar{n}_b^2 \left(\frac{1 - e^{-\Gamma_b t}}{\Gamma_b} \right)^2 + \frac{\bar{n}_b(2\bar{n}_b + 1)}{\Gamma_b} \left(te^{-\Gamma_b t} - \frac{1 - e^{-\Gamma_b t}}{\Gamma_b} \right) \right\}. \quad (\text{A13}) \end{aligned}$$

The Lorentzian center of the line shape is governed by the long-time limit of Eqs. (A7) and (A13),

$$\begin{aligned} K_1 &\rightarrow -i\delta\omega \bar{n}_b t, \\ K_2 &\rightarrow -\delta\omega^2 \frac{\bar{n}_b(\bar{n}_b + 1)}{\Gamma_b} t. \quad (\text{A14}) \end{aligned}$$

Inserting Eqs. (A14), (A5), and (A1) into Eq. (A4), then using Eqs. (17) and (19) lead to the result (24).

APPENDIX B

Here we evaluate the average

$$I(t) = \langle e^{-iA \int_0^t d\tau x_b^2(\tau)} \rangle, \quad (\text{B1})$$

where $x_b(\tau)$ is a Gaussian stochastic variable whose statistical properties are given by Eqs. (34) and (35). The n th term in the Taylor expansion of Eq. (B1) involves the average

$$\langle x_b^2(\tau_1) x_b^2(\tau_2) \dots x_b^2(\tau_n) \rangle \quad (\text{B2})$$

which may be represented as a sum of diagrams as follows: A preaveraged diagram of third order is shown in Fig. B1 and corresponds to the term

$$x_b^2(\tau_1) x_b^2(\tau_2) x_b^2(\tau_3), \quad (\text{B3a})$$

i.e., a vertex with two dashed lines corresponds to $x_b^2(\tau)$ (each vertex stands for a different time) and a full horizontal line i just a product operation. Averaging we obtain the unlinked and linked diagrams shown in Fig. B1 and corresponding to

$$\langle x_b^2(\tau_1) \rangle \langle x_b^2(\tau_2) \rangle \langle x_b^2(\tau_3) \rangle, \quad (\text{B3b})$$

$$\langle x_b(\tau_1) x_b(\tau_2) \rangle^2 \langle x_b^2(\tau_3) \rangle, \quad (\text{B3c})$$

$$\langle x_b(\tau_1) x_b(\tau_2) \rangle \langle n_b(\tau_2) x_b(\tau_3) \rangle \langle x_b(\tau_3) x_b(\tau_1) \rangle. \quad (\text{B3d})$$

Only linked diagrams contribute to the cumulant expansion. Using the appropriate weight factors corresponding to equivalent linked diagrams we get

$$I(t) = \exp \left\{ \sum_n \frac{2^{n-1} (-iA)^n}{n} \int_0^t d\tau_1 \dots \int_0^t d\tau_n K_n(\tau_1 \dots \tau_n) \right\}, \quad (\text{B4})$$

where K_n is the n th order linked diagram shown in Fig. B1:

$$\begin{aligned} K_n &= \langle x_b(\tau_1) x_b(\tau_2) \rangle \langle x_b(\tau_2) x_b(\tau_3) \rangle \\ & \times \dots \langle x_b(\tau_{n-1}) x_b(\tau_n) \rangle \langle x_b(\tau_n) x_b(\tau_1) \rangle. \quad (\text{B5}) \end{aligned}$$

Denote

$$\langle x_b(\tau) x_b(\tau') \rangle \equiv Z(\tau - \tau'). \quad (\text{B6})$$

Then from Eq. (35),

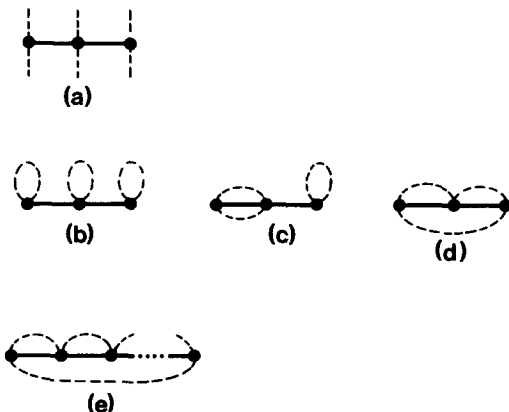


FIG. B1. Diagrams corresponding to various correlation functions involving the low frequency mode b (see Appendix B).

$$\hat{Z}(\omega) \equiv \frac{1}{2\pi} \int_{-\infty}^{\infty} dt e^{i\omega t} Z(t) = \frac{c}{(\omega_b^2 - \omega^2)^2 + \omega^2 \eta^2}. \quad (\text{B7})$$

Using Eqs. (B5) and (B7) we get

$$\begin{aligned} & \int_0^t d\tau_1 \dots \int_0^t d\tau_n K_n(\tau_1 \dots \tau_n) \\ &= \frac{1}{(2\pi)^n} \int_{-\infty}^{\infty} d\omega_1 \dots \int_{-\infty}^{\infty} d\omega_n \hat{Z}(\omega_1) \dots \hat{Z}(\omega_n) \\ & \times \int_0^t d\tau_1 e^{-i(\omega_1 - \omega_n)\tau_1} \int_0^t d\tau_2 e^{-i(\omega_2 - \omega_1)\tau_2} \\ & \times \dots \int_0^t d\tau_n e^{i(\omega_n - 1 - \omega_n)\tau_n} \xrightarrow{t \rightarrow \infty} \frac{t}{2\pi} \int_{-\infty}^{\infty} d\omega [\hat{Z}(\omega)]^n. \end{aligned} \quad (\text{B8})$$

Equations (B4) and (B8) now give

$$I(t) = \exp\left\{-\frac{t}{4\pi} \int_{-\infty}^{\infty} d\omega \ln[1 + 2iA\hat{Z}(\omega)]\right\} \quad (\text{B9})$$

which may be recast in the form

$$I(t) = e^{-i\Delta\omega t - 1/2\Gamma t}, \quad (\text{B10})$$

where

$$\begin{aligned} \Delta\omega &= \frac{1}{4\pi} \text{Im} \int_{-\infty}^{\infty} d\omega \ln[1 + 2iA\hat{Z}(\omega)] \\ &= \frac{1}{4\pi} \int_{-\infty}^{\infty} d\omega \arctan[2A\hat{Z}(\omega)], \end{aligned} \quad (\text{B11})$$

$$\begin{aligned} \Gamma &= \frac{1}{2\pi} \text{Re} \int_{-\infty}^{\infty} d\omega \ln[1 + 2iA\hat{Z}(\omega)] \\ &= \frac{1}{4\pi} \int_{-\infty}^{\infty} d\omega \ln\{1 + [2A\hat{Z}(\omega)]^2\}. \end{aligned} \quad (\text{B12})$$

There are Eqs. (40) and (41) ($A = \alpha/2\omega_a$).

APPENDIX C

In this Appendix, we will solve the differential equation (56),

$$xG'' + (1+x)G' + i(a+bx)G = e^{-x}. \quad (\text{C1})$$

Let us first write

$$G = e^{xc} g.$$

Substituting this in Eq. (C1) gives

$$\begin{aligned} xg'' + (1 + [2c + 1]x)g' + (c + ia + [c^2 + c + ib]x)g \\ = e^{-cx - x}. \end{aligned}$$

Now, choose

$$c^2 + c + ib = 0, \quad c = -\frac{1}{2}(1 + \sqrt{1 - 4ib}) \equiv -\frac{1}{2}(1 + w)$$

with $\text{Re } w > 0$. Thus

$$xg'' + (1 - wx)g' + (c + ia)g = e^{1/2(w-1)x}.$$

Next, substitute $wx = y$:

$$yg'' + (1 - y)g' + \frac{c + ia}{w}g = \frac{1}{w}e^{(w-1)y/2w}. \quad (\text{C2})$$

Now, note that ($n = \text{positive integer}$)

$$yg'' + (1 - y)g' + ng = 0 \quad (\text{C3})$$

has the Laguerre polynomials as solution

$$g = L_n(y) = \frac{1}{n!} e^y \frac{d^n}{dy^n} (e^{-y} y^n).$$

The Laguerre polynomials from a complete set of states which satisfies

$$\int_0^\infty dy e^{-y} L_n(y) L_m(y) = \delta_{nm} \quad (\text{C4})$$

and

$$\int_0^\infty dy e^{-Ay} L_n(y) = (A-1)^n A^{-n-1} \quad (\text{Re } A > 0). \quad (\text{C5})$$

Let us now expand the solution $g(y)$ to Eq. (C2) as

$$g = \sum_{n=0}^{\infty} g_n L_n. \quad (\text{C6})$$

We also write

$$\frac{1}{w} e^{(w-1)y/2w} = \sum_{n=0}^{\infty} a_n L_n, \quad (\text{C7})$$

where, using Eqs. (C4) and (C5),

$$a_n = \frac{2}{w+1} \left(\frac{1-w}{1+w}\right)^n.$$

Substituting Eqs. (C6) and (C7) in Eq. (C2) and using Eq. (C3) give

$$g_n = \frac{a_n}{(c + ia)/w - n}.$$

Finally, we must calculate

$$I(\omega) \sim \frac{1}{\eta} \text{Re} \int_0^\infty dx G(x, \omega).$$

We get

$$\begin{aligned} \int_0^\infty dx G &= \int_0^\infty dx e^{cx} g = \int_0^\infty dy \frac{1}{w} e^{cy/w} g \\ &= \sum_n \int_0^\infty dy \frac{1}{w} e^{cy/w} g_n L_n(y) = \sum_n \frac{2g_n}{1+w} \left(\frac{1-w}{1+w}\right)^n \\ &= \sum_{n=0}^{\infty} \frac{4}{(1+w)^2} \left(\frac{1-w}{1+w}\right)^{2n} \frac{1}{(c + ia)/w - n}. \end{aligned}$$

Thus

$$I(\omega) \sim -\text{Re} \left\{ \frac{4}{(1+w)^2} \sum_{n=0}^{\infty} \left(\frac{1-w}{1+w}\right)^{2n} \frac{1/\eta}{(c + ia)/w - n} \right\}.$$

Now, note that

$$\begin{aligned} \frac{1}{\eta w} \frac{1}{(c + ia)/w - n} &= \frac{-i}{\omega - \omega_a + i([2n + 1]w - 1)\eta/2} \\ &\equiv \frac{-i}{\omega - \omega_a - \Delta\omega_n + i\Gamma_n/2}, \end{aligned}$$

where

$$\Delta\omega_n - i\Gamma_n/2 = -\frac{i\eta}{2}([2n + 1]w - 1)$$

determines the frequency shift $\Delta\omega_n$ and linewidth (FWHM) Γ_n . One calculates easily

$$\Delta\omega_n = \pm \frac{(2n+1)\eta}{2\sqrt{2}} \left[(1 + [4\delta\omega n_b/\eta]^2)^{1/2} - 1 \right]^{1/2},$$

$$\Gamma_n = \eta \left[\frac{2n+1}{\sqrt{2}} (1 + [1 + (4\delta\omega n_b/\eta)^2]^{1/2})^{1/2} - 1 \right].$$

¹For reviews, See, Ph. Avouris and B. N. J. Persson, *J. Phys. Chem.* **88**, 837 (1984); J. W. Gadzuk and A. C. Luntz, *Surf. Sci.* **144**, 429 (1984).

²M. Trenary, K. H. Vram, F. Bozso, and J. T. Yates, Jr., *Surf. Sci.* **147**, 269 (1984).

³B. N. J. Persson and R. Ryberg *Phys. Rev. Lett.* **54**, 2119 (1985).

⁴B. E. Hayden and A. M. Bradshaw, *Surf. Sci.* **125**, 787 (1983).

⁵J. C. Tully, Y. J. Chabal, K. Raghavachari, J. M. Bowman, and R. R. Lucchese, *Phys. Rev. B* **31**, 1184 (1985).

⁶B. N. J. Persson (to be published).

⁷C. B. Harris, R. M. Shelby, and P. A. Cornelius, *Phys. Rev. Lett.* **38**, 1415 (1977); R. M. Shelby, C. B. Harris, and P. A. Cornelius, *J. Chem. Phys.* **70**, 34 (1979).

⁸The condition for validity of the WKB approximation is easily shown to be $(\alpha/4\omega_b^3 d/dt \langle x_b^2 \rangle) \ll 1$ and it holds because $\langle x_b^2 \rangle$ changes slowly on the ω_a time scale.

⁹Equation (46) is obtained by using $(\omega_b^2 - \omega^2) + \omega^2\eta^2 \rightarrow 4\omega_b^2(\omega - \omega_b)^2 + \omega_b^2\eta^2$. An additional factor of 2 results from the two peaks of $\hat{Z}(\omega)$, Eq. (42), near $\omega = \pm \omega_b$.